Article:
Martynov, S.B., Daud, N.K., Mahgerefteh, H. et al. (2016) Impact of stream impurities on compressor power requirements for CO2 pipeline transportation. International Journal of Greenhouse Gas Control. ISSN: 1750-5836

https://doi.org/10.1016/j.ijggc.2016.08.010

Impact of stream impurities on compressor power requirements for CO_2 pipeline transportation

S.B. Martynov, N.K. Daud, H. Mahgerefteh* , S. Brown[a], and R.T.J. Porter

Department of Chemical Engineering, University College London, London WC1E7JE

[a]*Current address*: Department of Chemical and Biological Engineering, University of Sheffield, Mappin Street, S1 3JDUK

*Corresponding author email: h.mahgerefteh@ucl.ac.uk

Abstract

The economic viability of Carbon Capture and Sequestration (CCS) as a means of mitigating CO_2 emissions is significantly dependent on the minimisation of costs associated with the compression and transportation of the captured CO_2. This paper describes the development and application of a rigorous thermodynamic model to compute and compare power requirements for various multistage compression strategies for CO_2 streams containing typical impurities originating from various capture technologies associated with industrial and power emission sectors. The compression options examined include conventional multistage integrally geared centrifugal compressors, supersonic shockwave compressors and multistage compression combined with subcritical liquefaction and pumping. The study shows that for all the compression options examined, the compression power reduces with the increase in the purity of the CO_2 stream, while the inter-stage cooling duty is predicted to be significantly higher than the compression power demand. For CO_2 streams carrying less than 5% impurities, multistage compression combined with liquefaction and subsequent pumping from *ca* 62 bar pressure can offer higher efficiency than conventional gas-phase compression. In the case of a raw/dehumidified oxy-fuel CO_2 stream of *ca* 85% purity, subcritical liquefaction at 62 bar pressure is shown to increase the cooling duty by *ca* 50% as compared to pure CO_2.

DOI: 10.1016/j.ijggc.2016.08.010

Keywords: CCS; CO_2 impurities; Oxy-fuel; Pre-combustion; Compression power; Cooling duty

1. Introduction

Carbon Capture and Sequestration (CCS) is a promising technology for mitigating the impact of anthropogenic CO_2 emissions from manufacturing industries and fossil fuel power generation on the global climate (Metz et al., 2005). An integral part of the CCS chain involves the transportation of the captured CO_2 to geological storage sites. Long-distance transportation of the large quantities of the captured CO_2 can be most efficiently achieved in the dense phase using pipelines at pressures typically above 86 bar (McCoy and Rubin, 2008). Given the relatively low pressure of CO_2 at the point of capture capture (Pei et al., 2014), its pipeline transportation requires additional upstream compression to reach the desired pressure.

It is estimated that the power demand for CO_2 compression can make up to 8-12 % to the cost of the electricity generated (Moore, et al., 2007). Therefore, the development of efficient schemes for the compression and conditioning of CO_2 prior to its transportation, and integration of these schemes within CCS is an important practical issue, attracting increasing attention (see for example, Ludke, 2004; Romeo et al., 2009; Aspelund and Jordal, 2007, Witkowski and Majkut, 2012; Moore et al., 2011).

In recent years, several types of industrial compressors, including in-line multiple-train and and integrally-geared centrifugal compressors currently employed in the natural gas processing industry, as well as novel two-stage supersonic and low-pressure axial compressors, have been considered for compression of CO_2 streams in CCS (Moore and Nored, 2008; IEAGHG, 2011). Particularly, analysis of conventional gas-phase multi-stage compression technology based on centrifugal compressors has shown that its efficiency can be increased by using a higher number of compression stages, combining compression with liquefaction and pumping, and applying liquefaction at lower

DOI: 10.1016/j.ijggc.2016.08.010

temperatures (IEAGHG, 2011). Comparing power consumption in centrifugal and supersonic compression of high-purity CO_2 streams from post-combustion capture has shown that (Witkowski and Majkut, 2012; Witkowski et al. 2013)the relatively low efficiency of supersonic shock-wave compressors can be compensated by utilising the compression heat in other processes in the plant, e.g., for regeneration of amine solutions or or preheating the boiler water. Pei et al. (2014) have performed analysis of waste heat recovery in CO_2 compression using an organic Rankine cycle, showing that the shockwave shockwave 2-stage compression consumes less energy than 7-stage centrifugal compression with intercooling.

While the above studies have primarily focused on the development of suitable compression strategies for high-purity CO_2, it has also been recognised that CO_2 streams in CCS inevitably carry some amount of impurities, whose nature and concentrations depend on the emission source and capture technology applied. In particular, combustion of coal and bio-mass derived fuels are expected to produce CO_2 streams carrying relatively large amount of impurities as compared to the natural gas fired plants. These impurities are expected to reduce the effective storage capacity of the reservoir and also affect the physical properties and vapour-liquid phase equilibrium of the CO_2 stream, directly impacting the design of compression equipment and the CO_2 pipeline transport (Goos et al., 2011). As such, several studies have attempted to quantify the effect of non-condensable gases on CO_2 compression. In particular, Li et al (2009) have concluded that power demand in single-stage gas-phase compression increases with the concentration of N_2, H_2, O_2 and Ar found in oxy-fuel derived CO_2. Similar conclusions have been made by Aspelund and Jordal (2007) who examined the variation in nitrogen content in a mixture on the compression power demand in direct gas-phase compression.

In order to minimise the compression costs associated with the presence of impurities in the CO_2 stream, several studies have focused on optimising the CO_2 separation and purification processes. In particular, Calado (2012) performed a model-based optimisation of the operation of compression trains for pre-combustion CO_2 streams, considering the pressure and temperature constraints imposed on the system due to

DOI: 10.1016/j.ijggc.2016.08.010

material considerations and dehydration process requirements. Posch and Haider (2012) modelled the double-flash separation and distillation-type compression-purification systems for oxy-fuel derived CO_2 streams captured in coal- and gas-fired power plants and compared the systems' power requirements with those employing conventional compression without purification. The study showed that using distillation allowed achieving CO_2 stream purity of *ca* 99.99%; much higher than in double-flash separation (*ca* 96%), but at a cost of significant increase (*ca* 30%) in the compression power duty.

While existing CO_2 separation technologies are capable of producing high-purity CO_2, these technologies can be energy demanding, hence the cost of purification should be balanced against the costs of transportation and storage of impure CO_2. de Visser et al (2008) have recommended that non-condensable gases, such as N_2 and Ar, which are not toxic and do not pose the risk of corrosion for the pipeline/ storage tank steel, can form up to 5% of the transported CO_2 stream, while not compromising the safety of pipeline transportation. At the same time, in the case of relatively small CO_2 emission sources, compression and transportation of low-grade CO_2 carrying more than 5% of impurities, may be required prior to its further purification. However, to date, the compression requirements for industrial low-grade CO_2 streams have not been systematically assessed.

In this paper, a rigorous thermodynamic model is developed and applied to compute and compare power consumption requirements for various multistage compression strategies including inter-stage cooling for impure CO_2 streams typical of CCS operations. The range and concentration of the typical impurities originating from various CO_2 capture technologies, as well as the relevant pressure and temperature conditions for the capture processes, are summarised in Section 2. Section 3 presents the CO_2 compression strategies evaluated in the study. Section 4 describes the thermodynamic model applied for calculating the power consumption for multi-stage compression. This is followed by presentation and discussion of the results in Section 5. Conclusions and recommendations for future work are presented in Section 6.

DOI: 10.1016/j.ijggc.2016.08.010

2. Industrial grade CO_2 streams

As mentioned in the introduction, CO_2 captured from coal and biomass fired plants is expected to contain larger amount of impurities as compared to gas-fired plants. This section provides a brief overview of the impurities found in CO_2 streams originating from coal combustion technologies. Table 1 provides a listing and typical concentrations of main fluid components found in CO_2 streams captured in post-combustion, pre-combustion and oxy-fuel processes. Given that the thermodynamic state of the CO_2 stream leaving the capture process is expected to have direct impact on the design and operation of the compression unit, conditions of CO_2 capture are briefly described for the three capture technologies following Porter et al. (2015).

2.1 Post-combustion capture

In post-combustion capture processes, CO_2 is separated from flue gas originating from air-fired combustion. Traditionally, amine-based absorption systems operating at close to ambient conditions [*ca* 1.5 bar and *ca* 40 ^{o}C (IEAGHG, 2011)] are used to capture the CO_2 from the flue gas, which typically contains only 5-15% v/v CO_2, with the remaining major components being O_2, N_2, Ar, H_2O, CO, NO_X and SO_2 (Table 1). Using amine-based solvents CO_2 can be purified to above 99% v/v. Due to its relatively high purity, the impact of impurities on thermodynamic properties of post-combustion CO_2 streams is often neglected (Witkowski et al, 2013).

2.2 Pre-combustion capture

In pre-combustion capture, coal is partially oxidised to produce syngas containing CO_2 which is then converted in a gas-shift reaction to CO_2 and H_2. CO_2 is next removed in an absorption process. After capture, the pre-combustion stream typically contains *ca* 98 % v/v CO_2, up to 1% v/v of N_2, H_2, CO, CH_4 , H_2O and Ar, and ppm level of acid gases (SO_2 and H_2S) (Table 1). In contrast to the post-combustion process, which starts from near-atmospheric pressure, in pre-combustion capture the flashing is achieved at pressures around 4.8 – 11.5 bar (IEA, 2011), whilst the Selexol absorption system operates at pressures from 20 to 130 bar (Oakey et al., 2010).

DOI: 10.1016/j.ijggc.2016.08.010

2.3 Oxy-fuel combustion capture

Among several capture processes, oxy-fuel combustion is considered as one of the most promising options which enables capturing the vast majority of CO_2 from coal-fired power plants and can be retrofitted to the existing fleet of modern pulverised coal-fired power plants (Tigges et al., 2009). In the oxy-fuel capture, the fuel is burned in a mixture of purified oxygen and recycled flue gas from the boiler containing mainly CO_2 and water vapour (Kownatzki and Kather, 2011). As a result, the oxy-fuel flue gas contains relatively high amounts of oxygen and water. Other major impurities include N_2 and Ar. Before dehumidification, the CO_2 concentration in oxy-fuel flue gas is around 70%. Water scrubbing is commonly achieved at ambient pressure to condense water vapour and remove traces of ash. Similar to pre-combustion capture, further purification of oxy-fuel derived CO_2 is performed in a sequence of steps at progressively increasing pressures. Removal of some reactive and soluble gases such as SO_3 and HCl can be achieved at pressures below 15 bar (White et al., 2006). At this stage, the increasing CO_2 stream has purity of *ca* 75-85 % v/v (see Table 1). Also, the 'sour compression' process proposed by Air Products allows reducing the removal SO_X and NO_X impurities (Allam et al, 2005). To further reduce the amount of non-condensable components (such as O_2, N_2 and Ar) and achieve CO_2 purity of over 95 % v/v, flash-evaporation and distillation are applied at pressures of *ca* 15-30 bar (Dillon et al., 2005; White et al., 2006, Besong et al., 2013).

3. CO_2 compression technology options

In practice, the choice and design of compressors is tailored to the conditions and scale of the CO_2 capture and transport. Several types of multistage compression technologies utilising various types of compressors have recently been considered for CO_2 compression. Table 2 summarises the three main technology options recommended for compression of high-purity CO_2 (Witkowski et al, 2013), which are in turn considered in the present study. The main features are briefly described below.

DOI: 10.1016/j.ijggc.2016.08.010

3.1 Option A: Centrifugal compressors

Option A is a conventional choice for CO_2 compression in the power generation industry (Aspelund, 2010). Given that the pressure ratio in a single-step centrifugal compressor is limited to 1.7-2 : 1 (Pei et al., 2014), reaching pressures of *ca* 150 bar requires using either integrally-geared or centrifugal compressors or trains of single-stage compressors, combined with the inter-stage cooling. Current designs of integrally-geared compressors use 8 to 10 stages to achieve pressures up to 150-200 bar (IEA GHG, 2011). In a recent study by Witkowski et al (2013), eight-stage centrifugal compressors were considered for compression of post-combustion CO_2 stream from 1.5 to 151 bar.

3.2 Option B: Supersonic shockwave compression

Option B, supersonic shockwave compression, is a novel technology uniquely suited for compression of large volumes of CO_2, offering compression efficiencies of more than 80% (Kidd and Miller, 2010). This option uses high pressure ratios, *ca* 10-12:1 per stage, and has more compact design and lower capital cost as compared to traditional centrifugal compression (option A). As an additional benefit, it provides the high discharge temperature of *ca* 279 ^{o}C, which can be utilised, for example for pre-heat of feed-water to the boiler or regenerating amine solutions in post-combustion capture applications (Witkowski et al., 2013). Recently, both two-stage and single-stage shock-wave compressors have been designed for processing of large amounts of CO_2 in CCS applications (Baldwin, 2009).

3.3 Option C: Compression combined with liquefaction and pumping

In compression combined with liquefaction and pumping, gas-phase centrifugal compressors are applied to raise the CO_2 pressure to an intermediate level, at which point, the CO_2 stream is liquefied and then pumped to a final pressure suitable for pipeline

DOI: 10.1016/j.ijggc.2016.08.010

transportation. The underlying premise of the liquefaction approach is that liquid pumps require significantly less power to raise pressure and are considerably less expensive than gas compressors (Duan et al., 2013). As such, liquefying and pumping at lower pressures could reduce the overall power demand for compression (Pei et al., 2014).

In practice, since at high pressures the boiling point of the pure CO_2 is close to the ambient temperature (at 62 bar the CO_2 saturation temperature is 23^{o}C), where applicable, conventional water cooling systems can be easily applied to liquefy CO_2. Depending on the cooling water temperature, using pumps to build up the fluid pressure from 62 to 150 bar allows saving of *ca* 10-20 % of the compression duty in conventional gas-phase compression (Aspelund, 2010; Witkowski and Majkut, 2012).

4. Methodology

4.1 Thermodynamic analysis

In the present study, a thermodynamic analysis method is applied to quantify the power consumption in multi-stage compression. The compression process is modelled as a sequence of idealised isentropic compression and isobaric cooling steps, ultimately converting the gas-phase CO_2 stream to the final dense-phase state ready for pipeline transportation.

The total power required for *N*-stage compression is given by:

$$W_{comp} = G \sum_{i=1}^{N} \frac{1}{\eta_{comp,i}} \int_{P_i^{in}}^{P_i^{out}} \left(\frac{dp}{\rho} \right)_s \qquad (1)$$

DOI: 10.1016/j.ijggc.2016.08.010

where, G and ρ are respectively the mass flowrate and the density of CO_2 stream, while p_i^{in}, p_i^{out} and $\eta_{comp,i}$ are respectively the inlet and outlet pressures and isentropic efficiency of the i-th stage. The subscript, *s* denotes isentropic compression.

Using the first law of thermodynamics, $dh = Tds + \frac{dp}{\rho}$ and assuming isentropic compression, equation (1) may be written as:

$$W_{comp} = G \sum_{i=1}^{N} \frac{1}{\eta_{comp,i}} \left(h_i^{out} - h_i^{in} \right) \tag{2}$$

where h_i^{out} and h_i^{in} are enthalpies of the stream at the suction (*in*) and discharge (*out*) of the i-th compression stage.

The total cooling duty associated with removing the heat of compression and possibly liquefying the CO_2 stream is given by:

$$Q_{cool} = G \sum_{i=2}^{N} \left(h_{i-1}^{out} - h_i^{in} \right) \tag{3}$$

In the present study the compression power and cooling duty are calculated as specific values per tonne of CO_2 captured, as commonly considered when estimating 'costs of CO_2 avoided' (Rubin et al., 2003). The corresponding specific compression power and cooling duty are defined as:

$$w_{comp} = \frac{W_{comp}}{G_{CO2}} = \frac{1}{\varphi_{CO2}} \frac{M_m}{M_{CO2}} \sum_{i=1}^{N} \frac{1}{\eta_{comp,i}} \left(h_i^{out} - h_i^{in} \right) \tag{4}$$

$$q_{cool} = \frac{Q_{cool}}{G_{CO2}} = \frac{1}{\varphi_{CO2}} \frac{M_m}{M_{CO2}} \sum_{i=2}^{N} \left(h_{i-1}^{out} - h_i^{in} \right) \tag{5}$$

DOI: 10.1016/j.ijggc.2016.08.010

where G_{CO2} and φ_{CO2} are respectively the mass flowrate and mole fraction of CO_2 component in a mixture, while M_m and M_{CO2} are molecular weights of the mixture and CO_2 respectively.

In order to estimate the power demand associated with cooling of the CO_2 stream, the approach is adapted based on calculating the work in an ideal compression refrigeration cycle moving the heat from a coolant evaporation temperature T_{ev} to a condensation temperature, T_{cond} (Jobson, 2014):

$$w_{cool} = \frac{q_{cool}}{\eta_{cool}} \left(\frac{T_{cond} - T_{ev}}{T_{ev}} \right) \tag{6}$$

were η_{cool} is the efficiency of refrigeration process. In the present study, the coolant evaporation temperature T_{ev} is set to be 5 ^{o}C less than the CO_2 stream cooling temperature, while the condensation temperature, T_{cond}, is assumed to be 38 ^{o}C.

4.2 Properties of CO_2 mixtures with impurities

In the present study to determine pertinent CO_2 mixture properties required for calculation of the fluid enthalpies in equations (1) to (5), the Peng-Robinson Equation of State (PR EoS) (Peng and Robinson, 1976) along with the appropriate mixing rules (Zhao and Li, 2014, Sandler, 1999, Ya and Sadus, 2000) is employed.

In particular, to determine the fluid enthalpy, *h*, and temperature at a given pressure and entropy, *s,* pressure-entropy flash calculations are performed by solving simultaneously the following two equations (Sandler, 1999):

DOI: 10.1016/j.ijggc.2016.08.010

$$h = h^{IG} + RT(Z-1) + \frac{1}{2\sqrt{2b_c}}\left[T\left(\frac{d(a_c\alpha)}{dT}\right) - a_c\alpha\right]\ln\left[\frac{ZRT + \left(1+\sqrt{2}\right)pb_c}{ZRT + \left(1-\sqrt{2}\right)pb_c}\right] \quad (7)$$

$$s = s^{IG} + R\ln\left(Z - \frac{pb}{RT}\right) + \frac{1}{2\sqrt{2b_c}}\frac{d(a_c\alpha)}{dT}\ln\left[\frac{ZRT + \left(1+\sqrt{2}\right)pb_c}{ZRT + \left(1-\sqrt{2}\right)pb_c}\right] \quad (8)$$

where, h^{IG} and s^{IG} are respectively the fluid enthalpy and entropy in ideal gas state. a_c, α and b_c are the fluid-specific parameters, p_c and T_c are respectively the fluid critical pressure and temperature. $Z = \frac{p}{\rho RT}$ is the fluid compressibility.

The derivative $\frac{d(a_c\alpha)}{dT}$ is defined as:

$$\frac{d(a_c\alpha)}{dT} = -0.45724\frac{R^2T_c^2}{P_c}\kappa\sqrt{\frac{\alpha}{TT_c}}\,. \quad (9)$$

In the present study, the above fluid properties are calculated using PR EoS implemented in REFPROP v.9.1 (Lemmon et al., 2013).

5. Results and discussion

The impurities present in the CO_2 stream directly impact the fluid phase thereby constraining the operating envelops of the compression and pumping units. Accordingly, the VLE behaviour for the typical industrial-grade CO_2 streams captured in post-combustion, pre-combustion and oxy-fuel capture processes as presented in Table 1 are examined first. Following this, the thermodynamic conditions matching the fluid phase requirements for the compression, liquefaction and pumping of various purity CO_2 streams are determined and the corresponding thermodynamic compression paths are constructed. This is then preceded by evaluation of the power requirements for multistage

DOI: 10.1016/j.ijggc.2016.08.010

compression of the CO_2 streams to a dense-phase state suitable for the pipeline transportation and storage.

5.1 VLE of impure CO_2 streams

To illustrate the variations in the phase equilibria of CO_2 streams of various purities, the liquid-vapour phase boundary is calculated for the mixture compositions from Table 1 using the PR EoS. Figure 1 shows the pressure-temperature phase diagram with the saturation line for pure CO_2 and the bubble-point and dew-point lines for the various CO_2 mixtures. As can be seen from Figure 1, the small amount of impurities in CO_2 mixtures produced in post-combustion CO_2 and distillation-grade oxy-fuel stream (99.3% v/v purity) has very little impact on the bubble-point and dew-point curves, which remain close to the saturation curve for pure CO_2. Notably, relatively small amount of hydrogen in the pre-combustion CO_2 stream (1.5% v/v) has nearly as strong impact on the phase equilibrium as that for 3.2% v/v of volatiles (N_2, O_2 and Ar) in oxy-fuel double-flash stream. In the case of raw oxy-fuel mixtures, which carry relatively large amounts of impurities (15% v/v), the bubble-point and dew-point pressures are remarkably different from the vapour pressure of pure CO_2. As can be seen from Table 1, the bubble-point temperature of post-combustion CO_2 stream at 62 bar is ca 23 ^{o}C, which reduces in the presence of impurities. In particular, the bubble-point temperature for the oxy-fuel derived 85% v/v CO_2 purity is *ca* – 55.4 ^{o}C, which is much lower than that for the other CO_2 streams (Table 1).

As the presence of impurities in oxy-fuel CO_2 stream shifts the VLE boundaries to higher pressures, it can be expected that higher pipeline operating pressures will be required to maintain the CO_2 in the dense phase. Also, the changes in the bubble point caused by the presence of impurities would affect the operating conditions for CO_2 stream liquefaction and pumping. As such, the knowledge of the VLE for the CO_2 stream is prerequisite for the design of compression strategies and should be considered when deciding on the compressor operating conditions as discussed in the following.

DOI: 10.1016/j.ijggc.2016.08.010

5.2 Multistage compression of CO_2 streams containing impurities

In the following, the impact of CO_2 impurities on the power demand for multistage compression is determined based for relevant pressure and temperature conditions and prescribed number of stages for the differed types of compressors presented in Table 2. Given relatively little impact of impurities on properties of post-combustion and distillation-grade oxy-fuel CO_2 streams carrying less than 15% v/v of impurities, these two streams are not considered further in the study, where the focus is made on the 96.7% v/v and 85% v/v CO_2 purity oxy-fuel streams and CO_2 mixture from pre-combustion capture.

Following Witkowski et al., (2013) the CO_2 stream temperature entering the compressor is set at 38 ^{o}C, which is higher than the cri-condentherm temperature of CO_2-rich mixtures, ensuring the gaseous state of the fluid. Furthermore, following Witkowski and Majkut (2012), it is assumed that each compression stage is followed by inter-stage cooling bringing the CO_2 stream back to 38 ^{o}C. It is also assumed that the CO_2 stream leaves the compression unit at 151 bar and 38 ^{o}C (except when combining compression with liquefaction and pumping as in the option C, as will be explained later). As discussed in Section 2, the oxy-fuel and pre-combustion CO_2 capture become most efficient at elevated pressures around 10-20 bar, which is achieved by coupling the compression and purification processes. Since this coupling complicates the analysis of the impact of impurities on compression, the present study is focused on the high-pressure compression phase starting from an intermediate pressure of 15 bar, which is chosen from the operating pressure range of oxy-fuel and pre-combustion capture technologies.

For the purpose of the present study, the pressure ratios for the individual stages of compression of the impure CO_2 streams is chosen based on the previous recommendations for the high-purity CO_2 (Witkowski et al, 2013). In particular, for multi-stage centrifugal compressors (option A), the pressure ratio is set to 1.78:1, while for the supersonic shock-wave compressors (option B), the pressure ratio is chosen to be

DOI: 10.1016/j.ijggc.2016.08.010

10:1. In the case of multi-stage compression (option C), following the strategy employed by Witkowski et al (2013), a 2-stage centrifugal compressor is utilised to raise the pressure in the gas stream from 15 to 62 bar, which is followed by subsequent liquefaction and pumping to 151 bar. As mentioned in Section 3.3, the advantage of the above compression strategy stems from the fact that using pumps is cheaper than operating compressors. However, in order to benefit from this advantage, the liquefaction should be achieved without significant rise in capital and operating costs. Also, in order to avoid formation of dry ice in a condensing gas, its temperature should remain above the triple point temperature of fluid, which in case of pure CO_2 is –56.6 ^{o}C. Table 2 shows that for all the CO_2 streams considered the liquefaction can be performed at 62 bar pressure and temperatures above –56.6 ^{o}C. As such, in the present study the liquefaction is assumed to be performed at 62 bar pressure which is only slightly above 60 bar pressure recommended for high-purity CO_2 (Witkowski and Majkut, 2012; Aspelund, 2010).

Figures 2, 3 and 4 respectively represent the fluid pressure-enthalpy *p-h* diagrams showing compression paths for the different compressor types A, B and C (Table 2) based on the above pressure ratios, inlet/outlet conditions and four CO_2 streams representative of the various capture technologies. The latter include 96.7% v/v and 85% v/v CO_2 purity oxy-fuel streams, pre-combustion stream carrying 98.07% v/v of CO_2, and pure CO_2, which practically represents high-grade post-combustion and distillation-grade CO_2 (Table 1).

Figure 2 *a* for pure CO_2 provides a reference for analysis of compression of impure CO_2 streams in Figures 2 *b, c* and *d*. Returning to Figure 2 *a*, the CO_2 *p-h* compression path corresponds to the 4-stage compression from the inlet 38 ^{o}C and 15 bar (point 0) to 38 ^{o}C and 151 bar final state (point 4). During each compression stage (*0-1, 1'-2, 2'-3, etc*), at the constant pressure ratio of 1.78:1, the exit fluid temperature reaches *ca* 90 ^{o}C. This temperature is then reduced to 38 ^{o}C in isobaric cooling processes (*1-1', 2-2', 3-3', etc*) before entry into the next compressor stage.

DOI: 10.1016/j.ijggc.2016.08.010

Figures 2 *b-d* show the phase diagrams and the fluid *p-h* compression paths for the three CO_2 mixture streams representative of the various capture technologies (Table 1). In each case, the 4 stage compression starts from 15 bar and 38 ^oC. In practice, the 4-stage compression is performed using either a specially designed high-pressure integrally geared compressor, or using the more conventional, though less compact, train of 4 single-stage compressors (IEAGHG, 2011).

Figures 3 *a-d* present the fluid phase boundaries and the corresponding *p-h* paths for the supersonic shock-wave compression of pure CO_2 (Figure 3 *a*) and the various CO_2 mixtures (Figures 3 *b-d*). In all the cases the inlet temperature and pressure are taken as 38 ^oC and 15 bar with a pressure ratio of 10:1 resulting in the final delivery pressure of 151 bar. Inter-cooling at each stage reduces the compressed fluid temperature from *ca* 279 ^oC back to the feed temperature of 38 ^oC. As discussed previously by Witkowski et al (2013), the shock-wave compressors consume more power than conventional centrifugal compressors, but offer more compact design, have lower capital cost and generate compression heat of sufficient quality to be utilised elsewhere in the plant.

Figures 4 *a-d* show the corresponding data as in Figures 3 *a-d* but for multistage compression with pumping following liquefaction of the CO_2 at subcritical pressures (option C, Table 2). As shown in Figure 4 *a* for pure CO_2, the feed is first compressed in 2 stages (*0-2*) from 1.5 bar to 62 bar, followed by isobaric liquefaction (*2-2'*), isothermal pumping to 151 bar (*2'-3'*) and heating back to the inlet temperature of 38^oC (*3'-4*). Similarly, in Figures 4 *b-d*, the three-stage compression of impure oxy-fuel and pre-combustion streams from 15 bar (*0-1-1'-2*) is followed by liquefaction (*2-2'*), pumping (*2'-3'*) and heating (*3'-4*).

5.3 Compression power requirements

Figure 5 shows the compression power demands, the inter-stage cooling duties and the cooling power demands per tonne of CO_2 captured, calculated using equations (4), (5) and (6) respectively, for the cases presented in Figures 2 - 4. Following the study by

DOI: 10.1016/j.ijggc.2016.08.010

Witkowski et al. (2013), the compressor efficiency is set to 0.8, while the cooling system efficiency is set to 0.6 (Jobson, 2014.). To account for high pressures of CO_2 streams in pre-combustion and oxy-fuel capture (as discussed in Section 2), the analysis is performed for the high-pressure compression phase starting from 15 bar and 38 ^{o}C.

Figure 5 *a* shows the variation of the calculated compression power demands for the different compressors against the CO_2 purity. The corresponding cooling duty requirements are presented in Figure 5 *b*, while Figures 5 *c* shows the estimated power demands for the cooling system operation.

As can be seen from Figures 5 *a* and *b*, the presence of impurities in the CO_2 stream affects both the compression power and the inter-stage cooling duty. In agreement with previous studies (Witkowski et al, 2013; IEAGHG 2011), the power demand for compression of pure CO_2 using supersonic compressors (option B) is estimated to be *ca* 50% higher than that for the centrifugal compression (option A). On the other hand using liquefaction and pumping (option C) reduces the compression power demand by *ca* 15% when compared to multi-stage centrifugal compressors (option A).

Also, the results in Figure 5 *a* show nearly equal power demands for compression of the double-flash 96.7% v/v purity oxy-fuel and the 98.07% v/v purity pre-combustion streams. This can be attributed to the fact that the pre-combustion CO_2 stream contains 1.5 % v/v of hydrogen (Table 1), which is relatively small compared to 3.2% v/v of volatiles (N_2, O_2 and Ar) found in oxy-fuel double-flash stream, but has stronger effect on the physical properties of the fluid, particularly the density and, hence, the compression power.

Remarkably, the results in Figure 5 indicate that multistage compression is characterised by a large cooling duty. In particular, when using compression options A, B and C to compress CO_2 streams carrying less than *ca* 5% (v/v) of impurities, the inter-stage cooling duty is predicted to be *ca* 3, 2 and 4 times bigger than the compression power (cf the data in Figures 5 *a* and *b*). This primarily can be attributed to non-ideal behaviour of

DOI: 10.1016/j.ijggc.2016.08.010

the CO_2 fluid and significant decrease in the fluid enthalpy with pressure, impacting the compression power and cooling duty in equations (4) and (5).

In the case of dehumidified oxy-fuel stream of 85% (v/v) purity, the cooling duty becomes particularly large, reaching *ca* 134 kWh/tCO_2, which can be attributed to relatively low temperature (-54.5 ^{o}C) considered for liquefaction of the 85% (v/v) purity oxy-fuel CO_2 stream. Possible strategies for removing such large amounts of heat from the CO_2 compression, may include optimising the heat integration between the CO_2 compression and other processes in the CCS plant.

The relatively large cooling duty in comparison with the compression power can be primarily attributed to a fact that at pressures above *ca* 15 bar the enthalpy of gas-phase CO_2 depends not only on temperature but becomes a strong function of pressure. As a result, the enthalpy increase in isentropic compression becomes less than the enthalpy decrease in the subsequent cooling to the original temperature. The latter can be illustrated by e.g. Figure 3 *a*, where the enthalpy changes in the compression (*0-1*) and cooling (*1-1'*) processes can be compared directly. It is important to note that actual power demand for operating the cooling system is not equivalent to the cooling duty and may be significantly reduced by integrating the cooling system operation with other processes in the CCS capture and CO_2 emission plant. Figures 5 c shows the estimates of power consumptions for operation of the cooling system as part of multistage compression process. From comparison of the data in Figure 5 a and 5c it can be seen that the cooling system is expected to consume less than ca 7% of power spend on compression in options A and B, while using compression option C (compression combined with liquefaction and pumping) results in significant increase in the cooling system power demand, which reaches *ca* 50% and 250% of the compression power when applied to oxy-fuel double-flash and the oxy-fuel dehumidified CO2 streams respectively.

While the minimum acceptable levels of impurities are dictated by specific transportation and storage conditions, the cost of CO_2 purification should be traded off against the costs of compression, transportation and storage of impure CO_2 stream. The results in Figure 5

DOI: 10.1016/j.ijggc.2016.08.010

a and *c* provide estimates for the power demand in compression per tonne of CO_2 avoided, which is relevant for analysis of the relative costs of mitigation of CO_2 emissions (Rubin, Rao and Chen, 2003).

Additionally, the relative changes in the compression power demand and cooling duties associated with the presence of impurities in CO_2 streams, are calculated as:

$$\delta w_{comp} = \frac{w_{comp} - w_{comp}^{CO2}}{w_{comp}^{CO2}} \cdot 100\% \quad (10)$$

$$\delta q_{cool} = \frac{q_{cool} - q_{cool}^{CO2}}{q_{cool}^{CO2}} \cdot 100\% \quad (11)$$

where w_{comp} and q_{cool} are respectively the specific compression power and cooling duty of impure CO_2 streams, while w_{comp}^{CO2} and q_{cool}^{CO2} are those corresponding to the pure CO_2.

Figures 6 *a* and *b* show respectively the relative changes δw_{comp} and δw_{cool}, calculated using equations (10) and (11) based on the data presented in Figure 5 for the CO_2 streams of various purity. As can be seen from Figure 6 *a*, the compression power generally increases with the decrease in CO_2 purity. This can be explained by the fact that compression power (see equation (2)) is inversely proportional to the fluid density which progressively decreases with the increase in the amount of the impurities. In the case of oxy-fuel stream carrying 85% v/v impurities, the multistage compression (Figure 6 *a*) demands *ca* 12-30% more power than compression of pure CO_2. Remarkably, the impact of CO_2 stream purity on the intercooling duty (Figure 6 *b*) is non-monotonic. In particular, when using compression options A and B, the impact of impurities on the cooling duty becomes notable only for the oxy-fuel CO_2 stream of 85% purity, where the cooling is reduced by less than *ca* 2% when compared to the pure CO_2. In the case of the compression option C, the cooling duty is slightly increased (by *ca* 5%) for pre-combustion and oxy-fuel double-flash streams, and becomes by *ca* 50% larger than

DOI: 10.1016/j.ijggc.2016.08.010

for the pure CO_2 when applied to oxy-fuel dehumidified CO_2 stream. The latter increase in the cooling duty can be attributed to the decrease in the bubble point temperature of the CO_2 mixture with the impurities as discussed earlier and as can be seen from the data in Table 1.

6. Conclusions and recommendations

The results of a thermodynamic analysis performed for determining the power requirements for the compression of CO_2 streams for pipeline transportation and subsequent geological sequestration were presented. The CO_2 streams considered included those captured from oxy-fuel and pre-combustion coal-fired power plants. Several industrial compression schemes as previously recommended for high-purity CO_2 streams captured in a post-combustion plant (Witkowski et al., 2013) were considered. The three strategies examined included gas-phase compression using multistage centrifugal compressors, multistage compression of CO_2 gas followed by liquefaction and pumping, and gas-phase compression using supersonic shock-wave two-stage and single-stage compressors. Given the relatively high pressures of CO_2 streams captured in oxy-fuel and pre-combustion processes, the analysis was performed for the high-pressure compression phase starting at 15 bar.

It was found that for oxy-fuel and pre-combustion CO_2 streams of purity higher than *ca* 96%, the compression power for the three compression strategies examined was not significantly affected by the presence of impurities. In case of the oxy-fuel stream with 85% CO_2 purity, the compression power requirement for the three compression schemes considered was found to increase by *ca* 12-30 % more than that for the compression of pure CO_2.

The power demand for operating the inter-stage coolers is estimated to be relatively small in comparison with the compression power demand (less than *ca* 7%) when using the centrifugal and shock-wave compressors. However, when using compression combined

DOI: 10.1016/j.ijggc.2016.08.010

with liquefaction and pumping, the cooling system operation can take up about 50% of the compression power when applied to the oxy-fuel double-flash and pre-combustion CO_2 streams, and becomes nearly 2.5 times higher than the compression power demand when applied to an oxy-fuel dehumidified stream of 85% CO_2 purity.

The relatively high estimated power demand for the operation of the compressor cooling system can be attributed to large cooling duties for the liquefaction of impure CO_2 streams. In particular, the cooling duty was shown to increase by up to 50% when compressing oxy-fuel CO_2 with 85% v/v purity as compared to that for pure CO_2.

Remarkably, for CO_2 streams of higher than 95 % v/v purity, compression combined with liquefaction and pumping can result in as much as *ca* 15% increase in efficiency as compared to conventional centrifugal compression. The liquefaction can be achieved at subcritical pressures around 62 bar using conventional water cooling systems at temperatures in the range 10 to 20 ^{o}C. At the same time, the study shows that operating such a system becomes less feasible for lower grade CO_2 streams due to incomplete liquefaction of the CO_2 stream. In particular, given the low bubble-point temperatures of oxy-fuel streams of *ca* 85% CO_2 purity, liquefaction at 62 bar would require using coolant temperatures as low as –54.5 ^{o}C which would not be economically viable. This temperature may be increased by applying CO_2 liquefaction at higher pressures, however, to determine the optimal conditions for the liquefaction, the trade-off between the costs for operating compressors and cooling/pumping system should be carefully considered.

Acknowledgements

DOI: 10.1016/j.ijggc.2016.08.010

The financial support from the European Union 7th Framework Programme FP7-ENERGY-2012-1-2STAGE under grant agreement number 309102 (CO2QUEST), the UK Engineering and Physical Science Research Council (UKCCSRC grant number UKCCSRC-C2-183) and from Ministry of Education, Malaysia is gratefully acknowledged.

References

ASPELUND, A. 2010. Carbon dioxide CO_2 compression, transport and injection processes and technology. *In:* MAROTO-VALER, M. M. (ed.) *Developments and Innovation in Carbon Dioxide (CO_2) Capture and Storage Technology: Carbon Dioxide (CO_2) Capture, Transport And Industrial Applications* Elsevier Woodhead Publishing Series

ASPELUND, A. & JORDAL, K. 2007. Gas conditioning-The interface between CO_2 capture and transport. *International Journal of Greenhouse Gas Control,* 1**,** 343-354.

BALDWIN, P. 2009. Low-cost, high-efficiency CO_2 compressors. *Carbon Capture Journal***,** 18-21.

BALDWIN, P. 2011. World's first supersonic CO_2 compression tect facility.

BALDWIN, P. & WILLIAMS, J. 2009. Capturing CO_2: gas compression vs. liquefaction.

BESONG, M. T., MAROTO-VALER, M. M. & FINN, A. J. 2013. Study of design parameters affecting the performance of CO_2 purification units in oxy-fuel combustion. *International Journal of Greenhouse Gas Control,* 12**,** 441-449.

CALADO, M. A. P. A. 2012. Modeling and design synthesis of a CCS compression train system via MINLP optimization.

DE VISSER, E., HENDRIKS, C., BARRIO, M., MØLNVIK, M. J., DE KOEIJER, G., LILJEMARK, S. & LE GALLO, Y. 2008. Dynamis CO_2 quality recommendations. *International Journal of Greenhouse Gas Control,* 2**,** 478-484.

DILLON, D. J., PANESAR, R. S., WALL, R. A., ALLAM, R. J., WHITE, V., GIBBINS, J. & HAINES, M. R. 2005. Oxy-combustion processes for CO_2 capture from advanced supercritical PF and NGCC power plant.

DUAN, L., CHEN, X. & YANG, Y. 2013. Study on a novel process for CO_2 compression and liquefaction integrated with the refrigeration process. *International Journal of Energy Research,* 37**,** 1453-1464.

GOOS, E., RIEDEL, U., ZHAO, L. & BLUM, L. 2011. Phase diagrams of CO_2 and CO_2–N_2 gas mixtures and their application in compression processes. *Energy Procedia,* 4**,** 3778-3785.

IEAGHG 2011. Technical specifications: Impact of CO_2 impurity on CO_2 compression, liquefaction and transportation (IEA/Con/13/213).

DOI: 10.1016/j.ijggc.2016.08.010

KATHER, A. & KOWNATZKI, S. 2011. Assessment of the different parameters affecting the CO_2 purity from coal fired oxyfuel process. *International Journal of Greenhouse Gas Control*.

KIDD, H. A. & MILLER, H. F. 2010. Engineer's Notebook. Compression solutions for CO_2 applications (traditional centrifugal and superonic technology).

KOWNATZKI, S. & KATHER, A. 2011. CO_2 Purity in Coal Fired Oxyfuel Processes. *2nd Oxy-Fuel Combustion Conference*. Yeppoon, Queensland, Australia.

LEMMON, E. W., HUBER, M. L. & MCLINDEN, M. O. 2013. NIST Standard Reference Database 23, NIST Reference Fluid Thermodynamic and Transport Properties - REFPROP, Version 9.1. *In:* APPLIED CHEMICALS AND MATERIALS DIVISION, N. I. O. S. A. T., BOULDER, COLORADO 80305 (ed.).

LI, H. & YAN, J. 2009. Evaluating cubic equations of state for calculation of vapor–liquid equilibrium of CO_2 and CO_2-mixtures for CO_2 capture and storage processes. *Applied Energy,* 86**,** 826-836.

LUDKE, K. H. 2004. *Process centrifugal compressors: Basics, function, operation, design and application*.

METZ, B., DAVIDSON, O., CONINCK, H. D., LOOS, M. & MEYER, L. 2005. IPCC special report on Carbon Capture and Storage. *In:* PRESS, C. U. (ed.).

MICHAEL, B. W. & JOHN, C. B. CO_2 capture via oxyfuel firing: Optimisation of a retrofit design concept for a refinery power station boiler. First National Conference on Carbon Sequestration May 15-17 2001 2001 Washington DC.

MOORE, J. J., LERCHE, A., DELGADO, H., ALLISON, T. & PACHECO, J. Development of Advanced centrifugal compressors and pumps for carbon capture and sequestration applications. The 40th Turbomachinery Symposium, 2011 Houston, Texas. 107-120.

PEI, P., KIRTIPAL BARSEA, ANDRES J. GILB & NASAHA, J. 2014. Waste heat recovery in CO_2 compression. *International Journal of Greenhouse Gas Control,* 30**,** 86-96.

PENG, D.-Y. & ROBINSON, D. B. 1976. A New Two-Constant Equation of State. *Industrial & Engineering Chemistry Fundamentals,* 15**,** 59-63.

PIESSENS, R., DE DONCKER-KAPENGA, E., ÜBERHUBER, C. W. & KAHANER, D. K. 1983. Quadpack, A Subroutine Package for Automatic Integration. *Springer Series in Computational Mathematics, Vol. 1.* Springer.

PIPITONE, G. & BOLLAND, O. 2009. Power generation with CO_2 capture: Technology for CO_2 purification. *International Journal of Greenhouse Gas Control,* 3**,** 528-534.

PORTER, R. T. J., FAIRWEATHER, M., POURKASHANIAN, M. & WOOLLEY, R. M. 2015. The range and level of impurities in CO_2 streams from different carbon capture sources. *International Journal of Greenhouse Gas Control,* 36**,** 161-174.

ROMEO, L. M., BOLEA, I., LARA, Y. & ESCOSA, J. M. 2009. Optimization of intercooling compression in CO_2 capture systems. *Applied Thermal Engineering,* 29**,** 1744-1751.

SANDLER, S. 1999. Chemical and engineering thermodynamics. *In:* WILEY (ed.). Wiley.

SEEVAM, P. N., RACE, J. M., DOWNIE, M. J. & HOPKINS, P. Transporting the Next Generation of CO_2 for Carbon, Capture and storage: The impact of impurities on

DOI: 10.1016/j.ijggc.2016.08.010

supercritical CO_2 pipelines. 7th International Pipeline Conference, 29 September-3 October 2008 2008 Calgary, Alberta, Canada. 1-13.
SINGH, L. K. Optimize compressor parameters for reduced inlet pressure and gas flow. GTL Technology Forum 2015, 2015 Norris Conference centers-City Center, Houston, Texas. 1-8.
SPERO, C. 2014. Callide Oxyfuel Project – Lessons Learned.
SULZER, P. 2010. Behavior of Centrifugal Pumps in Operation. *Centrifugal Pump Handbook (3rd Edition).* Elsevier.
WHITE, V., ALLAM, R. & MILLER, E. 2006. Purification of oxyfuel-derived CO_2 for Sequestration or EOR.
WITKOWSKI, A. & MAJKUT, M. 2012. The impact of CO_2 compression systems on the compressor power required for a pulverized coal-fired power plant in post-combustion carbon dioxide sequestration. *The Archieve of Mechanical Engineering,* LIX**,** 1-18.
WITKOWSKI, A., RUSIN, A., MAJKUT, M., RULIK, S. & STOLECKA, K. 2013. Comprehensive analysis of pipeline transportation systems for CO_2 sequestration. Thermodynamics and safety problems. *Energy Conversion and Management,* 76**,** 665-673.
WITKOWSKI, A., RUSIN, A., MAJKUT, M., RULIK, S. & STOLECKA, K. 2015. *Advances in carbon dioxide compression and pipeline transportation processes,* Springer.
YA, S. W. & SADUS, R. J. 2000. Equations of state for the calculation of fluid phase equilibria. *American Institute of Chemical Engineers Journal,* 46**,** 169-196.
YOO, B.-Y., CHOI, D.-K., KIM, H.-J., MOON, Y.-S., NA, H.-S. & LEE, S.-G. 2013. Development of CO_2 terminal and CO_2 carrier for future commercialized CCS market. *International Journal of Greenhouse Gas Control,* 12**,** 323-332.
ZHAO, Q. & LI, Y.-X. 2014. The influence of impurities on the transportation safety of an anthropogenic CO_2 pipeline. *Process Safety and Environmental Protection,* 92**,** 80-92.
ZIABAKHSH-GANJI, Z. & KOOI, H. 2012. An Equation of State for thermodynamic equilibrium of gas mixtures and brines to allow simulation of the effects of impurities in subsurface CO_2 storage. *International Journal of Greenhouse Gas Control,* 11**,** 1-14.

IEAGHG, 2011. Rotating equipment for carbon dioxide capture and storage, 2011/07, September, 2011

Jobson, M. 2014. Energy Considerations in Distillation. In: Gorak A, Sorensen E, eds. Distillation: Fundamentals and Principles. Oxford: Academic Press; 2014:225–270. doi:10.1016/B978-0-12-386547-2.00006-5.

Kather, A., Paschke, B., Kownatzki, S., 2013. CO2-Reinheit für die Abscheindung und Lagerung (COORAL): Prozessgasdefinition, Transportnetz und Korrosion. Final Report. Hamburg University of Technology.

DOI: 10.1016/j.ijggc.2016.08.010

E.C., 2011. Implementation of Directive 2009/31/EC on the Geological Storage of Carbon Dioxide Guidance Document 2: Characterisation of the Storage Complex, CO2 Stream – Composition, Monitoring and Corrective Measures, ISBN-13 978-92-79-19834-2.

Oakey J. 2010. The Effects of Impurities for Capture Technologies on CO2 Compression and Transport. Cranfield; 2010. doi:10.1165/rcmb.2011-0115OC.

Tigges KD, Klauke F, Bergins C, et al. Conversion of existing coal-fired power plants to oxyfuel combustion: Case study with experimental results and CFD-simulations. Energy Procedia. 2009;1(1):549–556. doi:10.1016/j.egypro.2009.01.073.

Rubin ES, Rao AB, Chen C. 2003. Understanding the Cost of CO2 Capture and Storage for Fossil Fuel Power Plants. Public Policy. 2003;(March):1–9.

DOI: 10.1016/j.ijggc.2016.08.010

Figure captions

Figure 1 Boundaries of VLE region in pressure-temperature phase diagram for pure CO_2, pre-combustion, post-combustion and oxy-fuel streams (85 and 96.7 % v/v CO_2) calculated using PR EoS.

Figure 2 Phase envelope boundaries and thermodynamic paths for the 'option A' compression of pure CO_2 (a), oxy-fuel CO_2 of 85 % v/v purity (b), oxy-fuel CO_2 of 96.70 % v/v purity (c), and pre-combustion CO_2 stream (d).

Figure 3 Phase envelope boundaries and thermodynamic paths for the 'option B' compression of pure CO_2 (a), oxy-fuel CO_2 of 85 % v/v purity (b), oxy-fuel CO_2 of 96.70 % v/v purity (c), and pre-combustion CO_2 stream (d).

Figure 4 Phase envelope boundaries and thermodynamic paths for the 'option C' compression of pure CO_2 (a), oxy-fuel CO_2 of 85 % v/v purity (b), oxy-fuel CO_2 of 96.70 % v/v purity (c), and pre-combustion CO_2 stream (d).

Figure 5 Power consumption in multistage compression (options A, B and C) of pure CO_2 and the CO_2 mixtures of various purity (Table 1). (a) – compression duty, (b) – inter-stage cooling duty, (c) – cooling power demand.

Figure 6 The relative variation in the compression power *(a)* and inter-stage cooling duty *(b)* caused by the presence of impurities in the CO_2 streams (options A, B and C).

DOI: 10.1016/j.ijggc.2016.08.010

Table captions

Table 1 Average compositions of CO_2 mixtures captured in oxy-fuel, pre-combustion and post-combustion technologies (Porter et al., 2015).

Table 2 Multistage compression options.

DOI: 10.1016/j.ijggc.2016.08.010

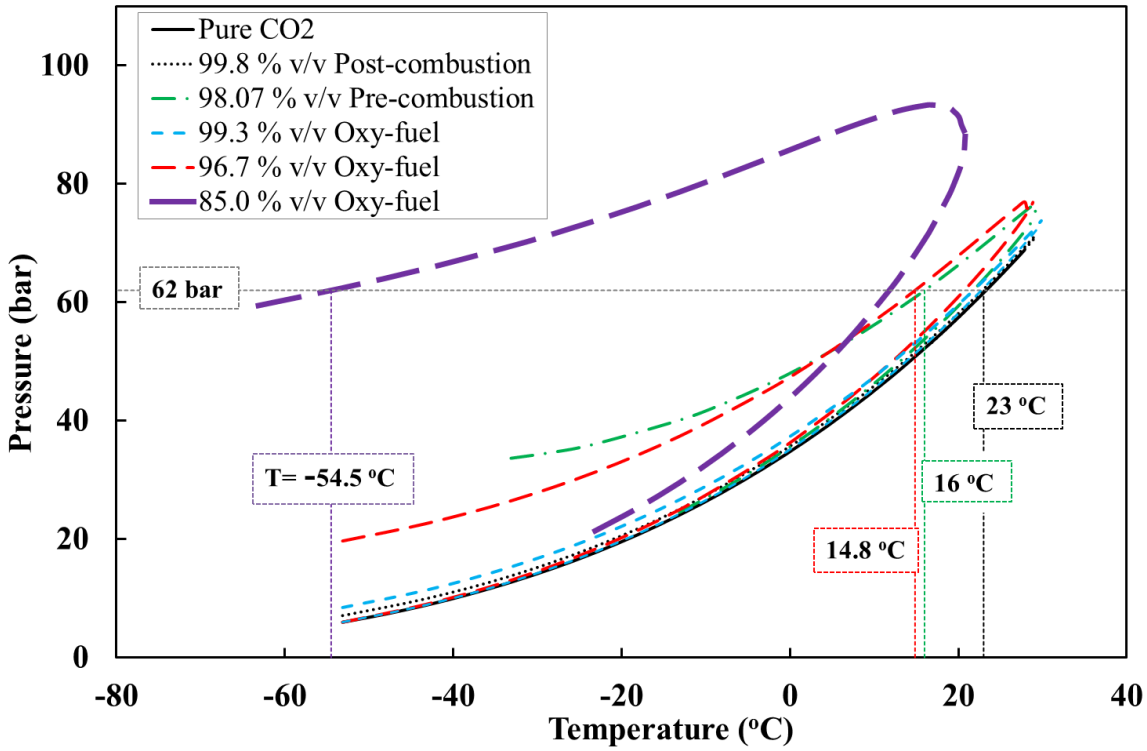

Figure 1:

DOI: 10.1016/j.ijggc.2016.08.010

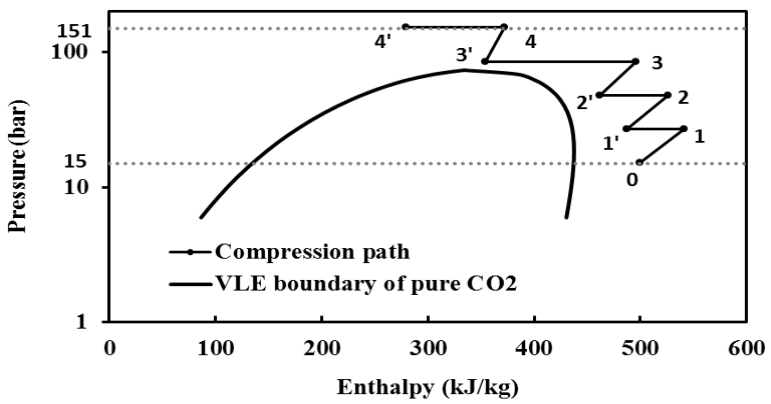

(a)

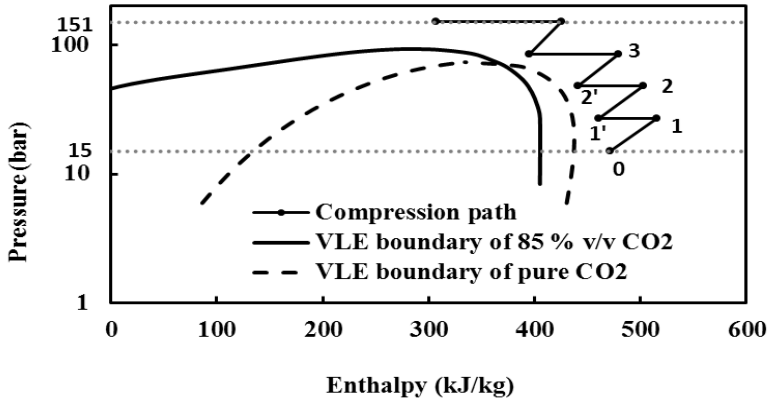

(b)

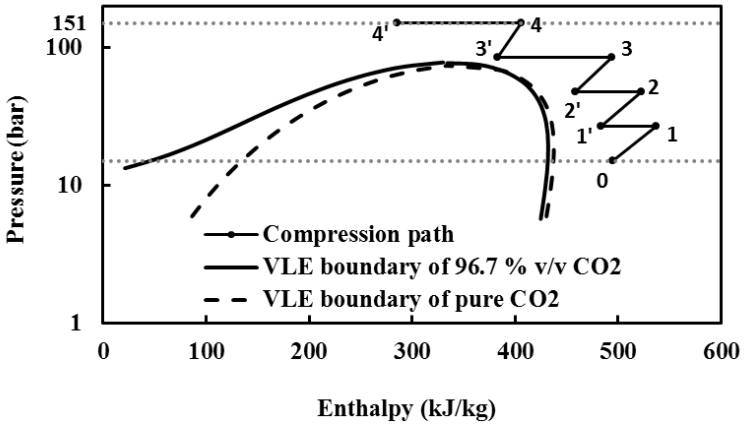

(c)

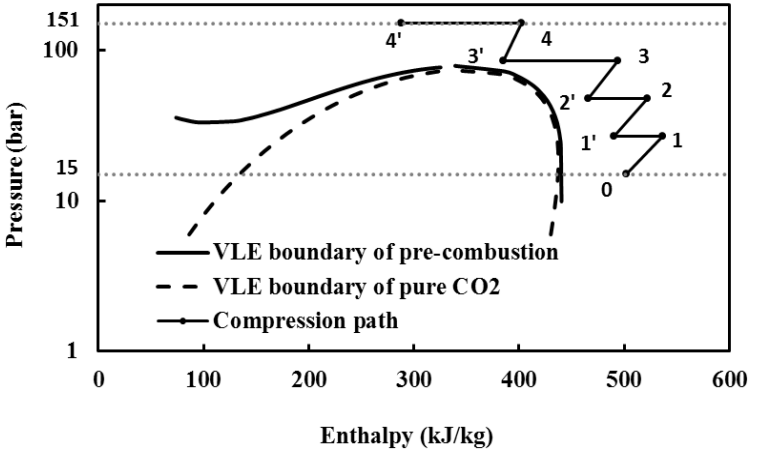

(d)

Figure 2:

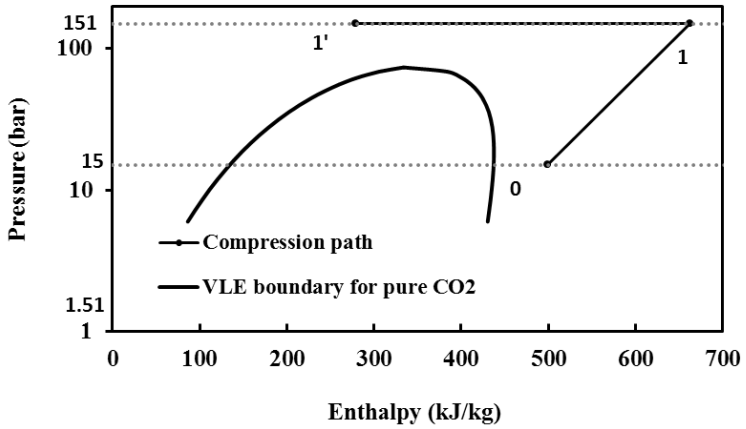

(a)

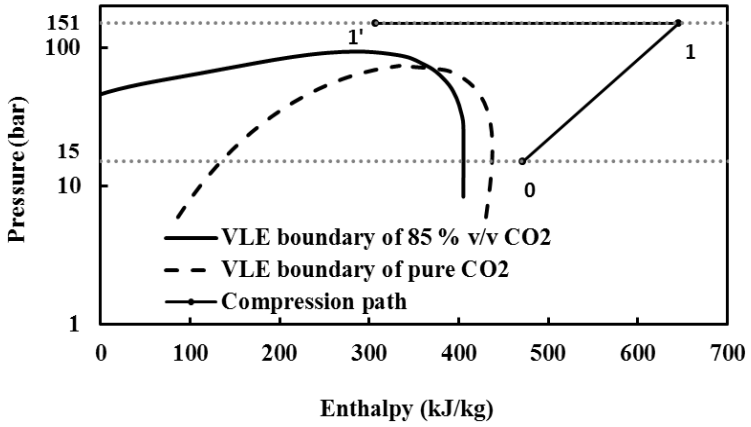

(b)

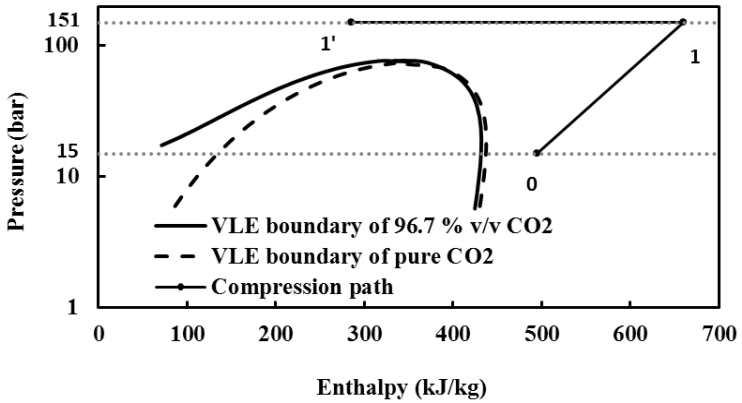

(c)

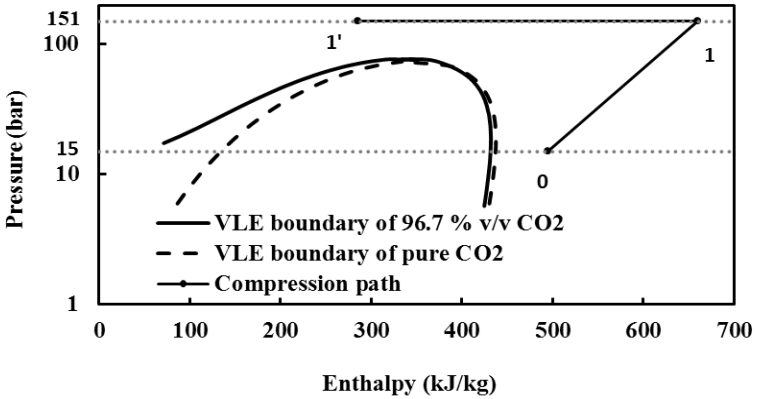

(d)

Figure 3:

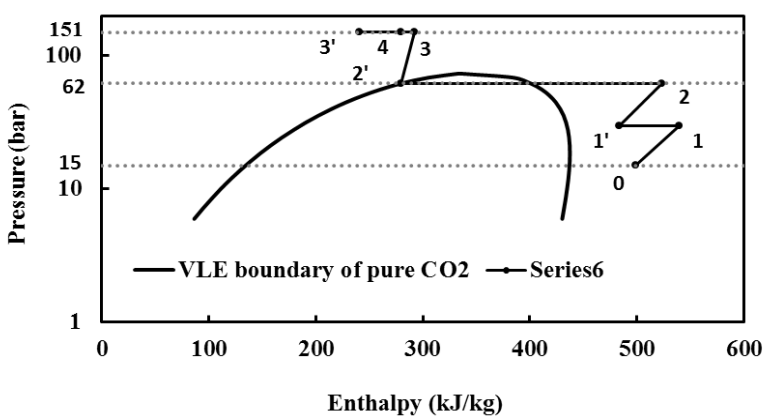

(a)

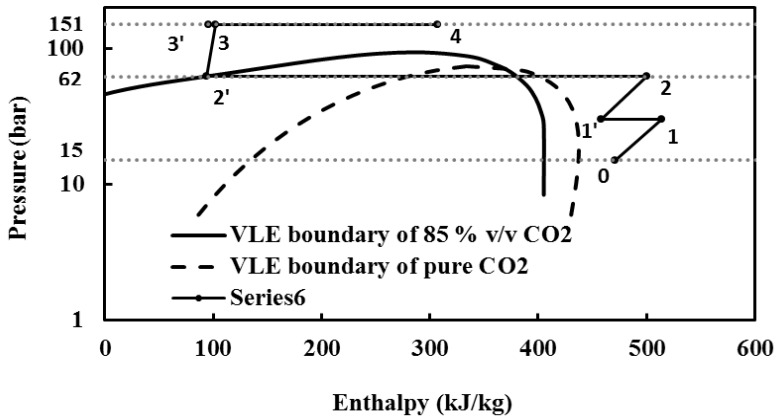

(b)

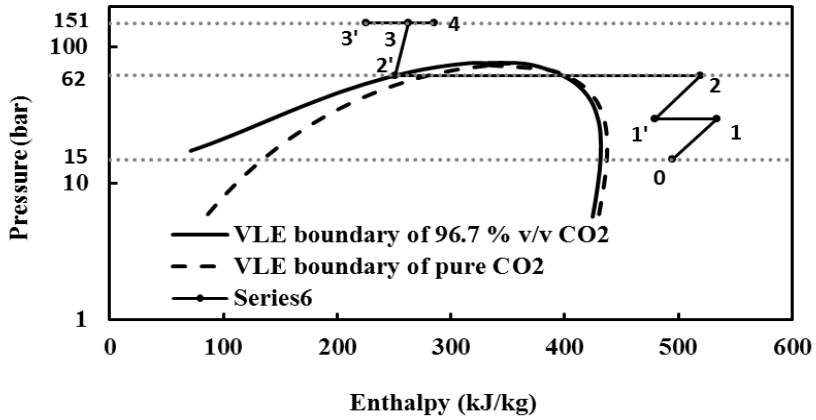

(c)

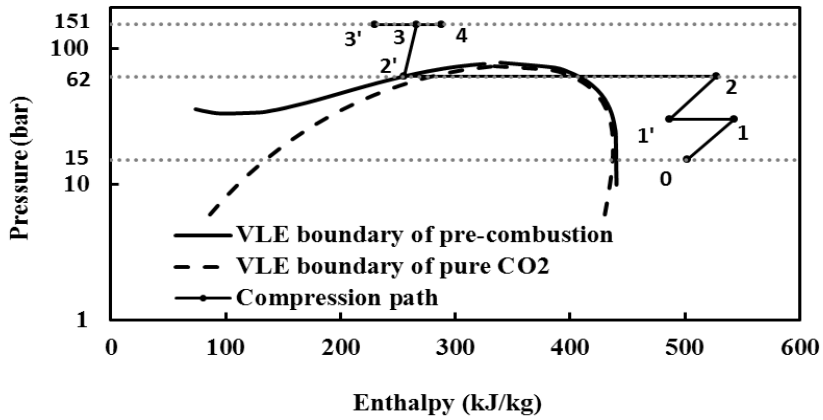

(d)

Figure 4:

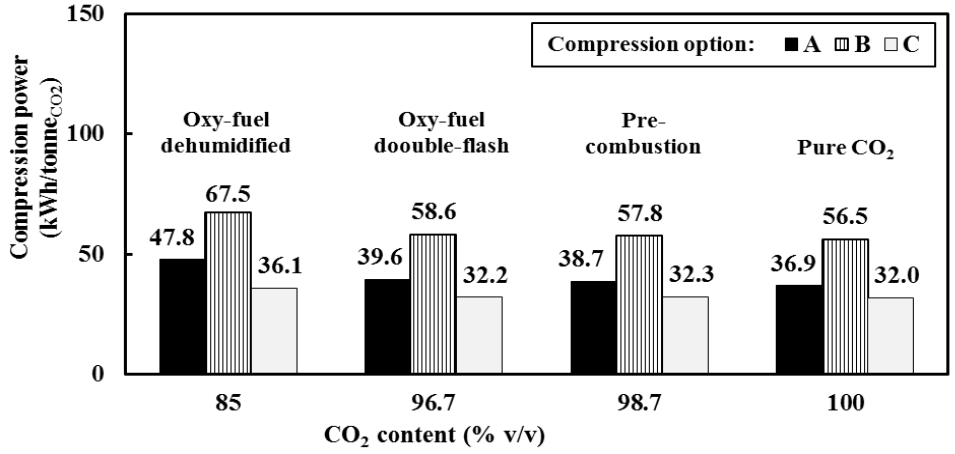
Compression option: A B C
Oxy-fuel dehumidified
Oxy-fuel doouble-flash
Pre-combustion
Pure CO2
Compression power (kWh/tonneCO2)
150
100
50
0
47.8
67.5
36.1
39.6
58.6
32.2
38.7
57.8
32.3
36.9
56.5
32.0
85
96.7
98.7
100
CO2 content (% v/v)

(a)

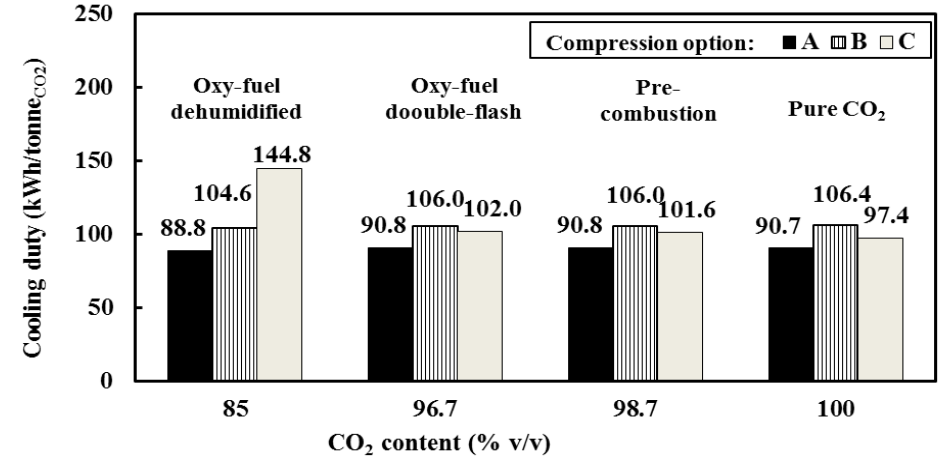
Compression option: A B C
Oxy-fuel dehumidified
Oxy-fuel doouble-flash
Pre-combustion
Pure CO2
Cooling duty (kWh/tonneCO2)
250
200
150
100
50
0
88.8
104.6
144.8
90.8
106.0
102.0
90.8
106.0
101.6
90.7
106.4
97.4
85
96.7
98.7
100
CO2 content (% v/v)

(b)

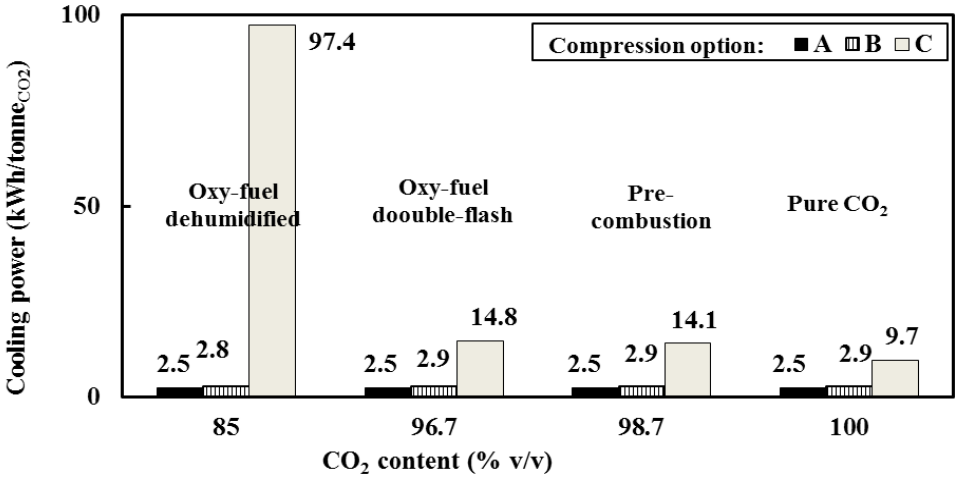
Compression option: A B C
Oxy-fuel dehumidified
Oxy-fuel doouble-flash
Pre-combustion
Pure CO2
Cooling power (kWh/tonneCO2)
100
50
0
2.5
2.8
97.4
2.5
2.9
14.8
2.5
2.9
14.1
2.5
2.9
9.7
85
96.7
98.7
100
CO2 content (% v/v)

(c)

Figure 5:

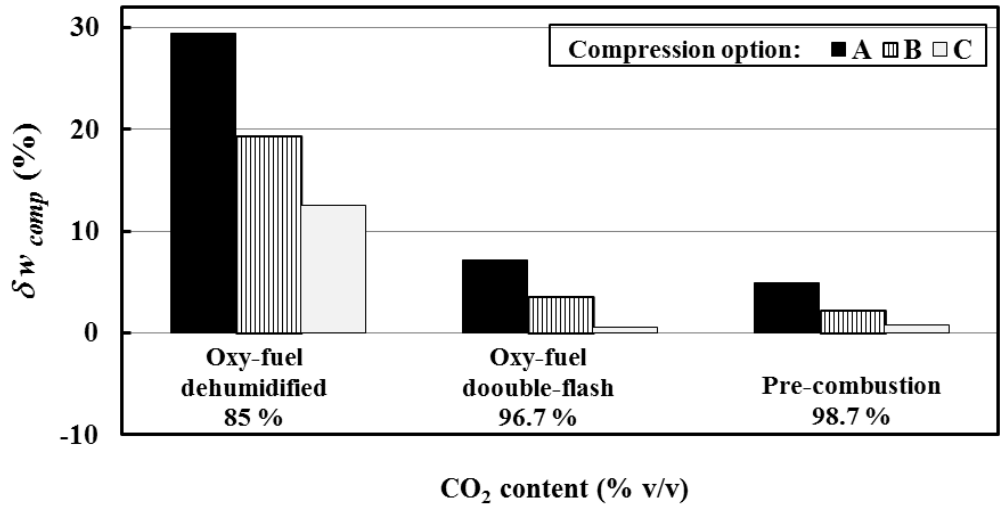
Compression option: A B C
30
20
10
0
-10
δw_{comp} (%)
Oxy-fuel dehumidified 85 %
Oxy-fuel doouble-flash 96.7 %
Pre-combustion 98.7 %
CO_2 content (% v/v)

(a)

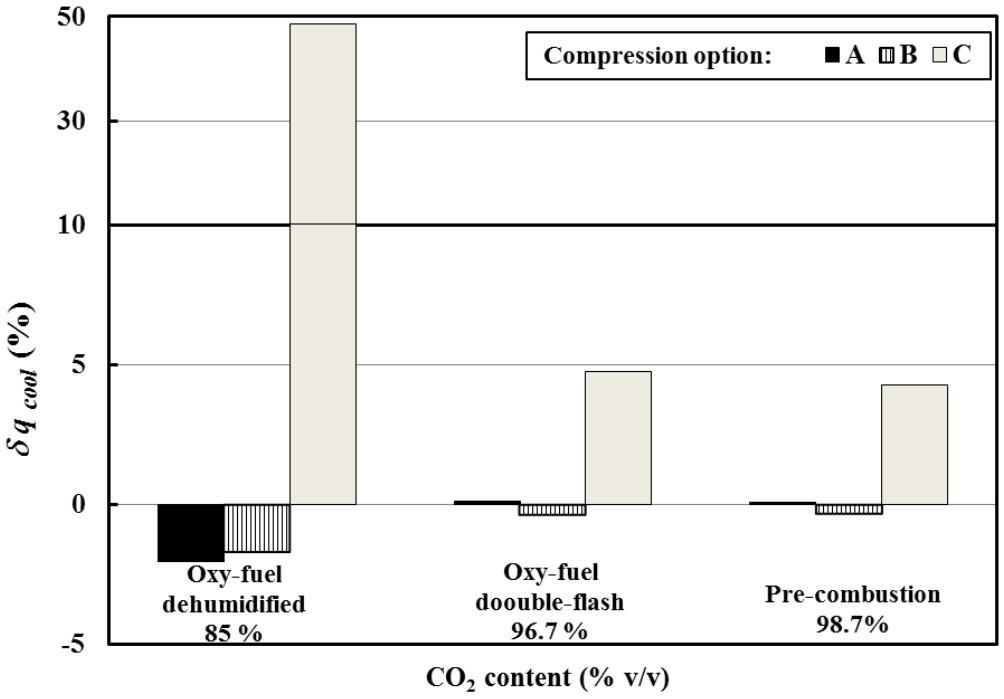
Compression option: A B C
50
30
10
5
0
-5
δq_{cool} (%)
Oxy-fuel dehumidified 85 %
Oxy-fuel doouble-flash 96.7 %
Pre-combustion 98.7%
CO_2 content (% v/v)

(b)

Figure 6:

Table 1:

	Oxy-fuel			Pre-combustion[c]	Post-combustion[d]
	Raw/ dehumidified[a]	Double flashing[b]	Distillation[b]		
CO_2 (% v/v)	**85.0**	**96.78**	**99.30**	**98.07**	**99.8**
O_2 (% v/v)	4.70	1.20	0.40	-	0.015
N_2 (% v/v)	5.80	1.60	0.20	0.02	} 0.045
Ar (% v/v)	4.47	0.40	0.10	0.018	
NO_x(ppm_v)	100	150	33	-	20
SO_2 (ppm_v)	50	36	37	700	10
SO_3(ppm_v)	20	-	-	-	-
H_2O(ppm_v)	100	-	-	150	100
CO (ppm_v)	50	-	-	1300	10
H_2S (ppm_v)	-	-	-	1700	-
H_2 (ppm_v)	-	-	-	15000	-
CH_4(ppm_v)	-	-	-	110	-
Bubble-point temperature (^oC) at 62 bar	-54.5	14.8	23	16	23

Sources: [a] (Kather and Kownatzki, 2011), [b] (Pipitone and Bolland, 2009), [c] (EC-2011), [d] (Kather et al, 2013).

Table 2:

Option	Type of compression machines
A	Multi-stage centrifugal compressors
B	Single- or two-stage supersonic shock-wave compressors
C	Multi-stage centrifugal compressors combined with the liquefaction and pumping units